



Supplement of

Simulating spatial multi-hazards with generative deep learning

Alison Peard et al.

Correspondence to: Alison Peard (alison.peard@ouce.ox.ac.uk)

The copyright of individual parts of the supplement might differ from the article licence.

S1 Comparison to Pareto GAN

Huster et al. (2021) investigated the ability of GANs to capture the extreme values of heavy-tailed data. In their experiments, they compared a classic GAN with Gaussian latents with their solution: ParetoGAN. ParetoGAN used heavy-tailed latents, a modified (non-adversarial) loss function, and applied power transforms to the generator’s output. The details of the original experiments are provided in full in (Huster et al., 2021).

Here we validate an alternative approach: rather than modifying the GAN to have heavy-tailed latents, we transform the training margins to a light-tailed (Gaussian) distribution, preserving agreement between the data and latent variable tails.

Table S1 shows the results for several experiments. The margins field specifies whether the original heavy-tailed (Cauchy to match Huster et al. (2021)) or Gaussian-transformed data was used. The Kolmogorov–Smirnov test statistic is defined as the largest magnitude difference between the distribution functions of two distributions and gives an indication of how well the *modes* of the data match. The area between of the log-log plots of the empirical survival functions of real and generated samples gives an indication of how well the generated *tails* match the real samples.

Table S1. Additional experimental results based on Huster et al. (2021)

Margins	Latents	Seed	KS statistic (\downarrow)	Log-log area (\downarrow)
Cauchy	Gaussian	1000	0.0141	54.6642
		1001	0.0185	54.5919
		1002	0.0133	52.9095
		Mean	0.0153	54.0552
Cauchy	Pareto	1000	0.0043	5.5712
		1001	0.0060	2.4611
		1002	0.0103	36.6845
		Mean	0.0069	14.9056
Gaussian	Gaussian	1000	0.0115	18.0198
		1001	0.0132	3.8996
		1002	0.0107	5.0781
		Mean	0.0118	8.9992

Figure S1 shows the tail distributions of the training (orange) and generated (blue) samples. Clearly, training heavy-tailed data with a Gaussian GAN under-represents the tails, but aligning the data and marginal tail weights leads to much-improved tail representation, whether it is achieved via ParetoGAN or transforming the heavy-tailed Cauchy training data.¹

¹The code to reproduce these results is available at <https://github.com/alisonpeard/paretogan>.

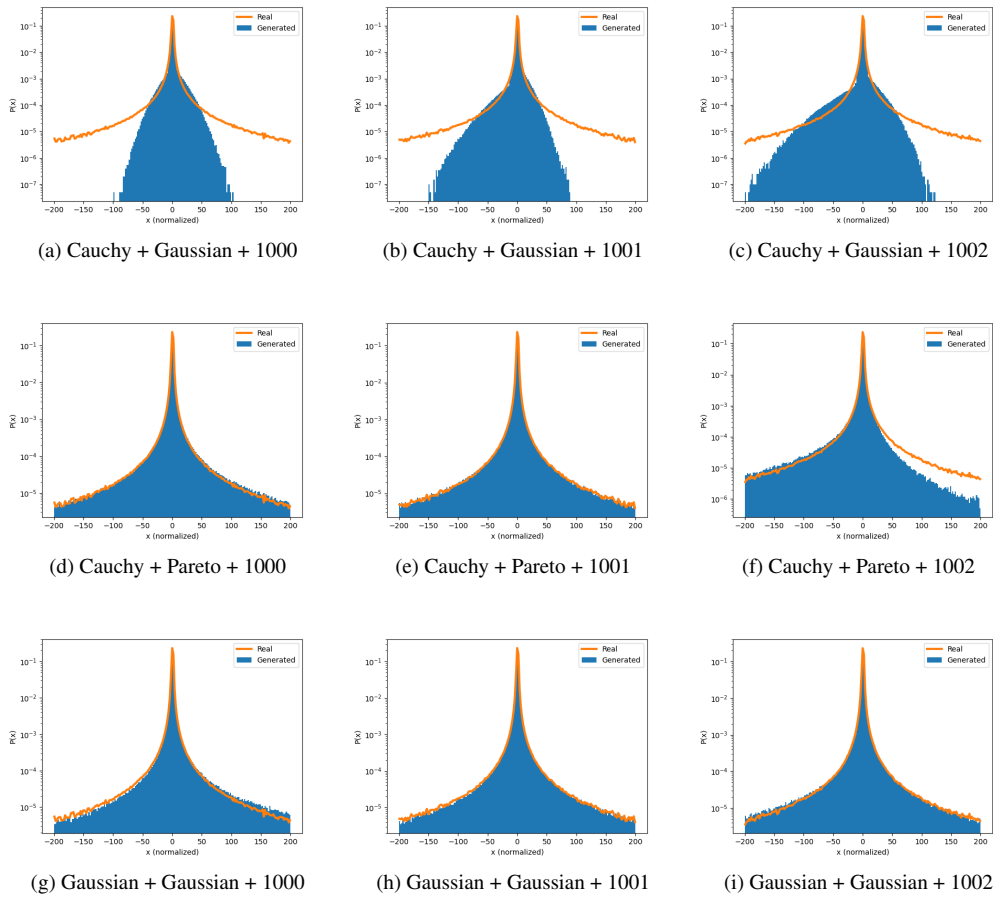


Figure S1. Tail distributions of real and GAN-generated samples. (Based on Huster et al. (2021).)

S2 Mangrove damage model

S2.1 Background

The Bay of Bengal is home to the Sundarbans mangrove forest, which provides habitats for over 5,000 plant and animal species (Spalding and Leal, 2024). Alongside habitat provisioning, mangroves provide many ecosystem services—coastal protection, carbon sequestration, and nutrient cycling (Krauss and Osland, 2020)—yet up to 30% of global mangrove extent has been lost in the past 50 years (Goldberg et al., 2020). While the main drivers of global mangrove losses are anthropogenic, natural disasters accounted for 3% of global mangrove losses between 2010 and 2020, almost entirely driven by disasters in Asia. This figure was three times greater than that of the previous decade. While mangroves in the Bay of Bengal are of less concern than mangrove systems elsewhere (Spalding and Leal, 2024), understanding the risk to these vital ecosystems remains important.

In terms of natural disasters, storms are a major driver of mangrove damage and dieback (Taillie et al., 2020; Goldberg et al., 2020; Bhatia et al., 2018). Mangrove forests sustain damages during storms via a range of interacting environmental, biological, and geophysical mechanisms (Mo et al., 2023; Taillie et al., 2020).

In recent studies, cumulative precipitation and maximum wind speed have been identified as strong predictors of storm damage to mangrove forests (Mo et al., 2023; Taillie et al., 2020; Amaral et al., 2023).

S2.2 Method

To simulate data under the independence assumption an independent standard uniform random variable is sampled for each pixel in the domain and this is transformed to data space using the probability integral transform from Sect. ???. The sampling procedure is repeated 914 times to generate an event set for the independence assumption. For the total dependence assumption, a percentile u_n is generated for each of a set of return periods RP_n according to,

$$u_n = 1 - \frac{1}{\lambda RP_n}.$$

The u_n value is broadcast across both the space (ij) and weather variable (k) dimensions and the return level at each (ijk)-combination is calculated using the PIT for that variable.

The mangrove vulnerability function is formulated as follows: we define a mangrove patch as “damaged” if it experiences a drop in enhanced vegetation index (EVI) greater than 20% in the wake of a storm. The logistic regression model is fitted to predict the probability of damage based on the maximum wind and cumulative precipitation near the mangrove patch during that storm. The fitted model achieves a precision score of 64%, recall of 70%, and a critical success index of 50%. The regression coefficient was 0.2961 for wind speed and 0.0975 for precipitation, indicating a strong and mild influence on damages by wind and precipitation, respectively. The historical weather fields in this model are derived from IBTrACS data, hence it is likely there will be some underestimation of damages when combining this model with ERA5 simulations, though this is somewhat alleviated by the damaged/not damaged binary model. Figure S2 visualises the bivariate response surface of the model. Mangrove presence data from Bunting et al. (2022) provides a shapefile of mangrove presence in the region. The Python ‘xagg’ package (Schwarzwald and Geil, 2024).

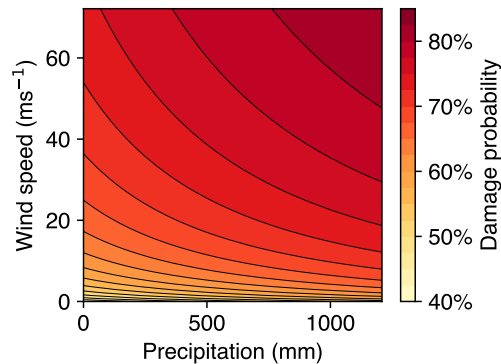


Figure S2. Bivariate response surface from logistic regression showing mangrove damage probability as a function of wind speed and precipitation, where mangrove damage is defined as a drop in EVI exceeding 20% in the wake of a storm.

The mangrove vulnerability function can now be applied to the historical ERA5 and synthetic storm footprints to predict damage probability fields for each wind storm event. To get the expected damage area (EDA)—the expected area of mangrove forest experiencing a drop in EVI greater than 20%—the damage probability field is multiplied by the area of mangroves present in each grid cell. Letting p be the probability the mangroves in a grid cell are damaged and assuming uniformity of damage probability within pixels,

$$\mathbb{E}[\text{damaged area}] = p \cdot [\text{mangrove area}] + (1 - p) \cdot [0] = p \cdot [\text{mangrove area}].$$

55 By linearity of the expectation function, we can also express the expected total area damaged (ETDA) for each storm as

$$\mathbb{E}[\text{total damaged area}] = \mathbb{E}\left[\sum_{i,j} \text{damaged area}_{i,j}\right] = \sum_{i,j} \mathbb{E}[\text{damaged area}_{i,j}].$$

We can now calculate the empirical distribution function \hat{F} over the set of ETDA's for each storm footprint. To obtain empirical return periods for each ETDA, we use the event occurrence rate $\lambda \approx 1.81$ to calculate return periods according to

$$\text{RP} = \frac{1}{\lambda(1 - \hat{F}(\text{ETDA}))}$$

60 where RP corresponds to a RP-year return period.

S3 Figures

S3.1 Precipitation and sea-level pressure footprints

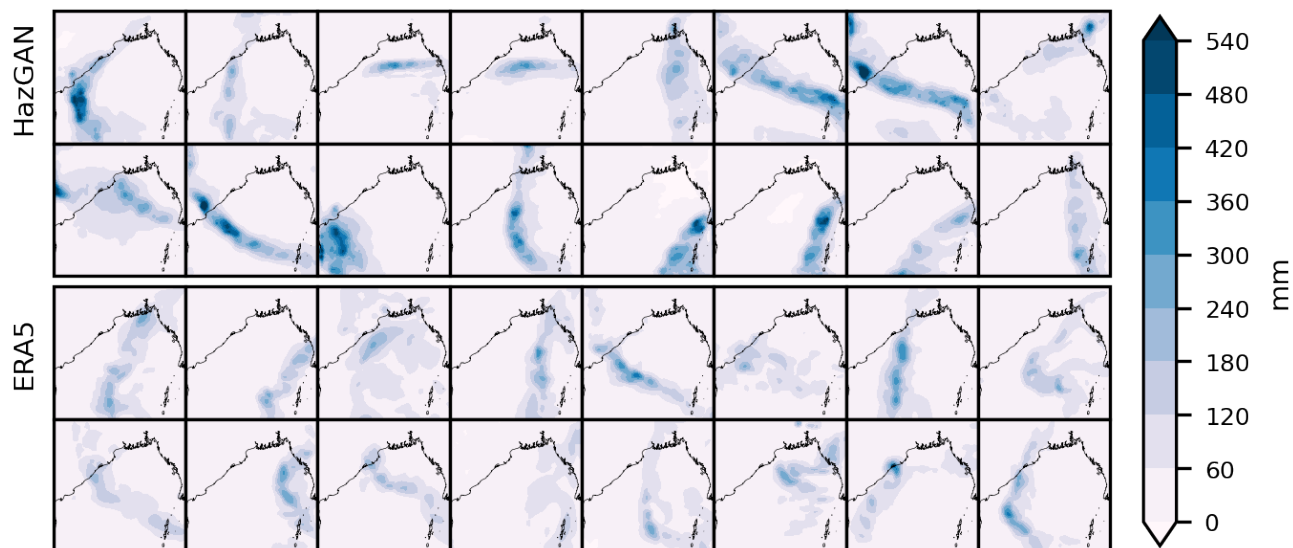


Figure S3. Comparison of generated (a) and training (b) precipitation fields over the Bay of Bengal. Generated fields are from the GAN trained on Gaussian margins (see main text).

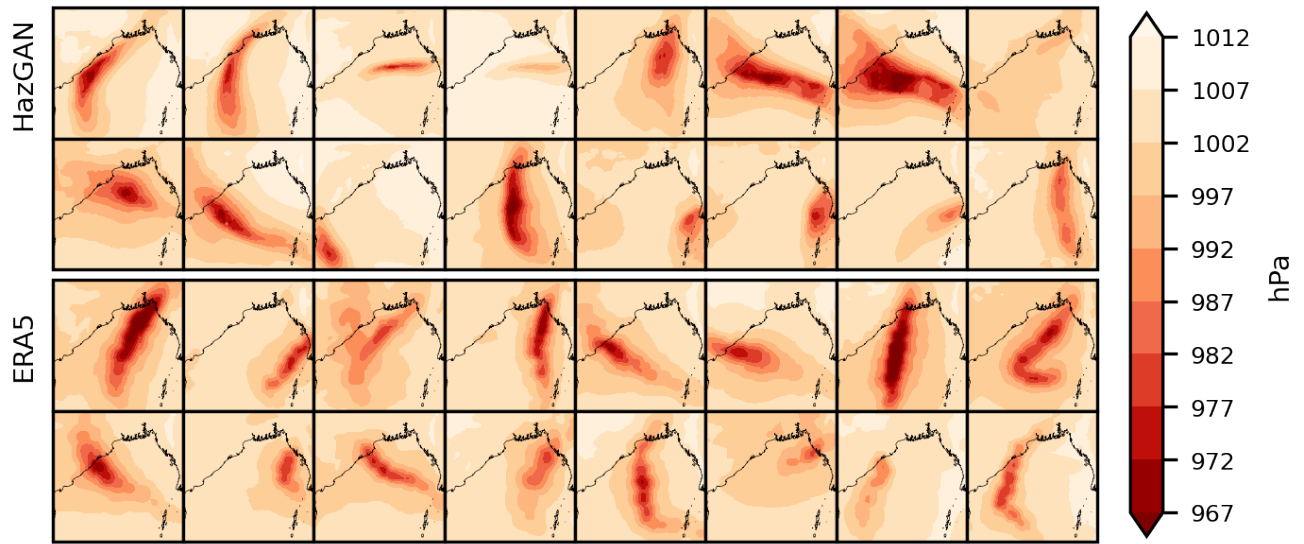


Figure S4. Comparison of generated (a) and training (b) atmospheric pressure fields in the Bay of Bengal. Generated fields are from the GAN trained on Gaussian margins (see main text).

References

- 65 Amaral, C., Poulter, B., Lagomasino, D., Fatoyinbo, T., Taillie, P., Lizcano, G., Canty, S., Silveira, J. A. H., Teutli-Hernández, C., Cifuentes-Jara, M., et al.: Drivers of mangrove vulnerability and resilience to tropical cyclones in the North Atlantic Basin, *Science of The Total Environment*, 898, 165413, 2023.
- Bhatia, K., Vecchi, G., Murakami, H., Underwood, S., and Kossin, J.: Projected response of tropical cyclone intensity and intensification in a global climate model, *Journal of climate*, 31, 8281–8303, 2018.
- 70 Bunting, P., Rosenqvist, A., Hilarides, L., Lucas, R., Thomas, T., Tadono, T., Worthington, T., Spalding, M., Murray, N., and Rebelo, L.-M.: Global Mangrove Extent Change 1996–2020: Global Mangrove Watch Version 3.0, *Remote Sensing*, 2022.
- Goldberg, L., Lagomasino, D., Thomas, N., and Fatoyinbo, T.: Global declines in human-driven mangrove loss, *Global change biology*, 26, 5844–5855, 2020.
- Huster, T., Cohen, J., Lin, Z., Chan, K., Kamhoua, C., Leslie, N. O., Chiang, C.-Y. J., and Sekar, V.: Pareto GAN: Extending the representational power of GANs to heavy-tailed distributions, in: *International Conference on Machine Learning*, pp. 4523–4532, PMLR, 2021.
- 75 Krauss, K. W. and Osland, M. J.: Tropical cyclones and the organization of mangrove forests: a review, *Annals of Botany*, 125, 213–234, 2020.
- Mo, Y., Simard, M., and Hall, J. W.: Tropical cyclone risk to global mangrove ecosystems: potential future regional shifts, *Frontiers in Ecology and the Environment*, 21, 269–274, 2023.
- 80 Schwarzwald, K. and Geil, K.: xagg: A Python package to aggregate gridded data onto polygons, *Journal of Open Source Software*, 9, 7239, <https://doi.org/10.21105/joss.07239>, 2024.
- Spalding, M. D. and Leal, M.: *The State of the World’s Mangroves 2024*, 2024.
- Taillie, P. J., Roman-Cuesta, R., Lagomasino, D., Cifuentes-Jara, M., Fatoyinbo, T., Ott, L. E., and Poulter, B.: Widespread mangrove damage resulting from the 2017 Atlantic mega hurricane season, *Environmental Research Letters*, 15, 064010, 2020.